

An Extended One-Ring MIMO Channel Model

Min Zhang, Peter J. Smith, and Mansoor Shafi

Abstract—In this paper we develop a Multiple Input Multiple Output (MIMO) channel model and derive its spatial and temporal correlation properties. We present a generalized methodology to derive the spatial correlation when the angles of arrival (AoA) and angles of departure (AoD) are either independent or partly correlated. Our model therefore spans the full range from well-established single ring models, where AoA and AoD are fully correlated to complex industrial channel models where they are uncorrelated. It is shown that first order and second order approximations to the channel give rise to a single-Kronecker model and a sum-Kronecker model respectively. We compare our model to other MIMO channel models in terms of correlation structure and the ergodic mutual information (EMI) and study the effect of the non-Kronecker correlation structure.

Index Terms—MIMO, channel models, mutual information, Kronecker model.

I. INTRODUCTION

THE number of MIMO channel models available in the literature is rapidly growing [1]–[5] and their complexity is increasing [5], [6]. Many of these models have the now well-known Kronecker form [1], [3], [4] and result from the assumption of separate scattering mechanisms at the base station (BS) and the mobile station (MS). In this paper we refer to this form as a “single-Kronecker” structure to differentiate it from an alternative form we call a “sum-Kronecker” structure. We refer to a sum-Kronecker structure when the correlation matrix can be expressed as the sum of two or more Kronecker products. Although a single-Kronecker model is popular and shows good agreement with some measured data [3], [7], its accuracy has been questioned [4], [8]–[10]. These papers propose that the single-Kronecker model is mainly suitable for MIMO systems with small number of antenna elements and it underestimates the ergodic mutual information (EMI) when compared to measurement data. Commonly used one-ring models [1], [2], [11], [12] are by their nature “non-Kronecker,” since the scattering mechanisms are linked. For these one-ring models, the angle of departure of a ray uniquely determines the angle of arrival. This observation motivates the development of a model which will bridge the gap between one-ring models, where AoD and AoA are fully correlated,

and models where AoD and AoA may only be loosely related and a single-Kronecker structure is plausible.

In this paper, we develop such a model, always bearing in mind a desire for mathematical simplicity, physical reality and ease of generation. The model builds on the approach proposed by Abdi and Kaveh [2]. Two approximations to the new model are studied which give particularly simple single-Kronecker and sum-Kronecker structures. The new model is then compared to standard one-ring models and Kronecker models. The EMI of the MIMO link is also considered and we show the relationship between EMI, antenna orientation and the level of correlation between AoD and AoA.

The main contributions of the paper are the following. An extension of the one-ring model is developed which allows for varying degrees of correlation between AoA and AoD. An approximation of this model provides a simple sum-Kronecker structure which is more general than the traditional single-Kronecker format. New results are also presented for the spatial correlation at the BS which agree with SCM132 [5] but decay more rapidly and with less oscillation than the correlation predicted by one-ring models. Finally, we discuss the effect of non-Kronecker correlation structures on EMI. We show that non-Kronecker correlation does not necessarily increase the EMI as previously reported [11], [12]. Note that although the results presented here assume a uniform distribution for the direction of motion of the MS, the model itself has no such restriction.

II. MIMO LINK MODEL AND SPATIAL/TEMPORAL CORRELATION FUNCTIONS

In [7] it was shown that the single-Kronecker model accurately represents the general scattering environment when AoA and AoD are independent. Using the single-Kronecker model gives rise to virtual separation between AoA and AoD even when the actual communication link between AoA and AoD is inseparable, i.e. correlated. Hence, in this section we present a model which caters for channels with varying degrees of correlation between AoA and AoD, ranging from non-correlated to fully correlated. The model is further approximated by a sum-Kronecker form where the number of Kronecker products in the sum determines the accuracy of the approximation.

A. Model Interpretation

Let us consider the downlink of an (n_t, n_r) wireless MIMO system with n_t BS and n_r MS omnidirectional antenna elements, shown in Fig. 1. Here the BS is the transmitter and the MS is the receiver. The MS is surrounded by a large number of local scatterers with a given distribution. The relationship between the link distance D and the radius of the scatterer ring R is determined by Δ , that is $\tan(\Delta) = R/D$.

Manuscript received August 29, 2005; revised October 15, 2006 and April 16, 2007; accepted May 22, 2007. The associate editor coordinating the review of this paper and approving it for publication was M. Buehrer.

M. Zhang is with the Department of Information Engineering, The Australian National University, Canberra ACT 0200, Australia (email: min.zhang@rsise.anu.edu.au).

P. J. Smith is with the Department of Electrical and Computer Engineering, The University of Canterbury, Private Bag 4800 Christchurch, New Zealand (email: p.smith@elec.canterbury.ac.nz).

M. Shafi is with Telecom New Zealand, PO Box 293, Wellington, New Zealand (email: Mansoor.Shafi@telecom.co.nz).

Digital Object Identifier 10.1109/TWC.2007.05659.

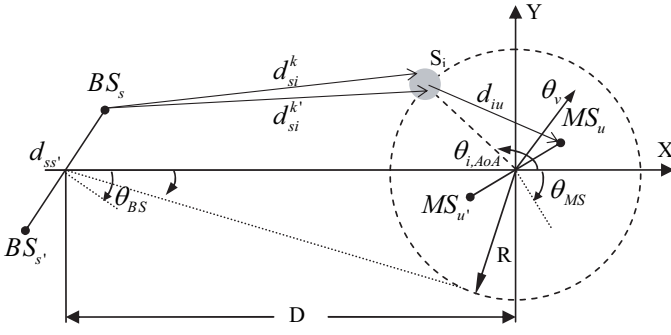


Fig. 1. Schematic diagram of the new MIMO channel model for a downlink system.

We will assume that $D \gg R$. The MS moves with speed v and the direction of motion is θ_v . The ring of scatterers is assumed to be fixed so that the accuracy of the spatial-temporal correlations given by the model are most reliable for short periods of time ($\ll R/v$). We do not consider line-of-sight (LOS) in the system since one of our main aims is to analyze the separability of the channel correlation structure and a LOS path fundamentally ties the MS and BS effects. For example, McNamara et al. [13] have found the single-Kroneckerstructure to be reasonable only under NLOS propagation.

In our model, each AoA is not associated with one specified AoD as in one-ring models [2], instead, an AoA is associated with a cluster of M subpaths (AoDs) with given power azimuth spectrum (PAS). Physically, we assume that a particular subpath leaves the s^{th} array element BS_s in the direction of $\theta_{i,AoD}^k$, which is defined as the angle between the k^{th} subpath and the x -axis, impinging on the u^{th} array element, MS_u , in the direction of $\theta_{i,AoA}$ after being scattered by S_i and combining. We only model a single ray at the MS which can be interpreted as a sum over subrays from scatterer S_i .

B. The General Spatial-Temporal Correlation Function

For the downlink system in Fig. 1, a mathematical representation for the propagation model is given below, using a similar derivation to that in [2],

$$h_{su}(t) = \lim_{N \rightarrow \infty} \lim_{M \rightarrow \infty} \sum_{i=1}^N g_i \left\{ \sum_{k=1}^M g_i^{(k)} \exp \left(j\psi_i^k - \frac{j2\pi d_{si}^k}{\lambda} \right) \right\} \times \exp \left(-\frac{j2\pi d_{iu}}{\lambda} + j2\pi f_D \cos(\theta_{i,AoA} - \theta_v)t \right) \quad (1)$$

where $h_{su}(t)$ is the channel coefficient and $\mathbf{H}(t) = (h_{su}(t))$ is the channel matrix. Other parameters in (1) are defined below. N is the number of scatterers, g_i is the wave amplitude of the i^{th} path where $\sum_{i=1}^N \|g_i\|^2 = 1$ as $N \rightarrow \infty$. Each path is the sum of M subpaths; $g_i^{(k)}$ is the wave amplitude of the k^{th} subpath of the i^{th} path where $\sum_{k=1}^M \|g_i^{(k)}\|^2 = 1$ as $M \rightarrow \infty$. The two power normalizations ensure that the mean power of the channel coefficient is unity. Note that the g_i amplitude refers to the single path from scatterer i to the MS. The $g_i^{(k)}$ amplitudes relate to the M sub-paths from the

BS to the scatterer. ψ_i^k are the phase shifts introduced by the scatterers and are assumed to be independent and identically distributed (iid) uniform variables over $[0, 2\pi)$. d_{si}^k and d_{iu} are the distances from BS_s to S_i and from S_i to MS_u respectively. Finally, $f_D = v/\lambda$ is the maximum Doppler shift. As in [2], the summation over many paths leads to a Gaussian channel coefficient and so we have a Rayleigh channel.

For a fixed direction of motion, θ_v , we define the temporal-spatial correlation function for the channel coefficients as $\rho_{su,s'u'}(\tau, \theta_v) = E[h_{su}(t)h_{s'u'}^*(t + \tau)]$. We note that $E[\exp(j\psi_i^k - j\psi_{i'}^{k'})] = 1$ for $i = i'$ and $k = k'$ and is zero otherwise. Therefore, $\rho_{su,s'u'}(\tau, \theta_v)$ can be written as

$$\rho_{su,s'u'}(\tau, \theta_v) = \lim_{N \rightarrow \infty} \lim_{M \rightarrow \infty} \sum_{i=1}^N E[g_i^2] \times \left\{ \sum_{k=1}^M E[(g_i^{(k)})^2] \exp \left(-\frac{j2\pi}{\lambda} (d_{si}^k - d_{s'i}^{k'}) \right) \right\} \times \exp \left(-\frac{j2\pi}{\lambda} (d_{iu} - d_{i'u'}) - j2\pi f_D \cos(\theta_{i,AoA} - \theta_v)\tau \right) \quad (2)$$

In (2), the spatial and temporal correlations are intertwined. Hence it can not be simply broken down into a product of temporal, transmit and receive terms.

C. The Correlation Function Assuming a von Mises PAS

Now we use the von-Mises PAS at both ends following [2], [14]. The von Mises PAS is given by

$$f(\theta) = \frac{\exp[\kappa \cos(\theta - \bar{\theta})]}{2\pi I_0(\kappa)}, \quad \theta \in [-\pi, \pi] \quad (3)$$

where I_0 is the zeroth-order modified Bessel function and κ controls the width of angle spread (AS) defined as the root mean square of the angles. In fact, the AS, in radians, equals $1/\sqrt{\kappa}$ for large κ , with $\kappa = 0$ giving a uniform spread of angles over 360° (104° AS) and $\kappa = \infty$ giving a ray at the single angle $\bar{\theta}$. Note that (3) has a different interpretation at the two ends. At the BS, the PAS refers to the sub-paths from the source to a scatterer. Hence, κ_{BS} controls the spread of the sub-paths. At the MS end, κ_{MS} controls the spread of the scatterers as it refers to the paths received at the MS, one from each scatterer.

$\bar{\theta}$ is the mean direction and signals coming from this direction have maximum power assuming the von Mises PAS. Hence, $\bar{\theta}_{AoA}$ represents the direction of the strongest incoming wave from the N scatterers seen by the user. Moreover, $\bar{\theta}_{i,AoD}$ is the mean value of $\theta_{i,AoD}^k$ and is also the direction of the strongest incoming sub-path seen from a specified scatterer S_i , which can be determined by $\theta_{i,AoA}$. As $D \gg R$ and $\Delta \approx R/D$ is small, $\bar{\theta}_{i,AoD}$ can be simplified as below [2]

$$\bar{\theta}_{i,AoD} \approx \sin(\bar{\theta}_{i,AoD}) \approx R/D \sin(\theta_{i,AoA}) \approx \Delta \sin(\theta_{i,AoA}) \quad (4)$$

Using (4) it suffices to specify $\bar{\theta}_{AoA}$ and κ_{MS} , since these parameters allow $\theta_{i,AoA}$ to be generated and this gives $\bar{\theta}_{i,AoD}$. Hence, it is not necessary to specify $\bar{\theta}_{i,AoD}$.

In order to determine the power of any path or subpath, consider that the infinitesimal power comes from the differential angle $d\theta$ and its corresponding power distribution function,

$f(\theta)$, so that $E[(g_i)^2] = f(\theta_i)d\theta_i$ [2]. Hence, the power of every path or subpath with the von Mises PAS and the approximation (4) is given by

$$\begin{aligned} E[(g_i)^2] &= \frac{\exp[\kappa_{MS} \cos(\theta_{i,AoA} - \bar{\theta}_{AoA})]}{2\pi I_0(\kappa_{MS})} d\theta_{i,AoA} \\ E[(g_i^{(k)})^2] &= \frac{\exp[\kappa_{BS} \cos(\theta_{i,AoD}^k - \bar{\theta}_{i,AoD})]}{2\pi I_0(\kappa_{BS})} d\theta_{i,AoD}^k \\ &\approx \frac{\exp[\kappa_{BS} \cos(\theta_{i,AoD}^k - \Delta \sin(\theta_{i,AoA}))]}{2\pi I_0(\kappa_{BS})} d\theta_{i,AoD}^k \end{aligned} \quad (5)$$

The larger the value of κ_{BS} , the narrower the cluster of subpaths will be and the power of these subpaths will concentrate around the mean direction. As $\kappa_{BS} \rightarrow \infty$, they will converge into one ray and make AoA and AoD fully correlated. In other words, the larger the value of κ_{BS} , the higher the correlation between AoA and AoD.

Further simplification occurs under the sensible physical scenario where $D \gg d_{ss'}$ and $R \gg d_{uu'}$ [15] and $d_{ss'}$, $d_{uu'}$ are the distances between BS antennas s and s' and between MS antennas u and u' respectively. In this situation, using Fig. 1, we have

$$\begin{aligned} \frac{2\pi}{\lambda}(d_{si}^k - d_{s'i}^k) &\approx D_{ss'} \sin(\theta_{i,AoD}^k - \theta_{BS}) \\ \frac{2\pi}{\lambda}(d_{iu} - d_{iu'}) &\approx D_{uu'} \sin(\theta_{i,AoA} - \theta_{MS}) \end{aligned} \quad (6)$$

where $D_{ss'} = 2\pi d_{ss'}/\lambda$ and $D_{uu'} = 2\pi d_{uu'}/\lambda$ are the distances between the antenna elements in wavelengths. Substituting equations (5) and (6) into (2) and defining $D_t = 2\pi f_D \tau$, the correlation averaged over AoA and AoD can be expressed as

$$\begin{aligned} \rho_{su,s'u'}(\tau, \theta_v) &\approx \frac{1}{2\pi I_0(\kappa_{BS})} \frac{1}{2\pi I_0(\kappa_{MS})} \int_{-\pi}^{\pi} \int_{-\pi}^{\pi} \\ &\exp\{-jD_{ss'} \sin(\theta_{i,AoD}^k - \theta_{BS}) \\ &\quad + \kappa_{BS} \cos(\theta_{i,AoD}^k - \Delta \sin(\theta_{i,AoA}))\} \\ &\exp\{-jD_{uu'} \sin(\theta_{i,AoA} - \theta_{MS}) \\ &\quad + \kappa_{MS} \cos(\theta_{i,AoA} - \bar{\theta}_{AoA})\} \\ &\exp\{-jD_t \cos(\theta_{i,AoA} - \theta_v)\} d(\theta_{i,AoA}) d(\theta_{i,AoD}^k) \end{aligned} \quad (7)$$

Since Δ is small, we are able to use the approximations, $\cos(\Delta \sin(\theta_{i,AoA})) \approx 1$ and $\sin(\Delta \sin(\theta_{i,AoA})) \approx \Delta \sin(\theta_{i,AoA})$, in (7). This gives

$$\begin{aligned} \rho_{su,s'u'}(\tau, \theta_v) &\approx \frac{1}{2\pi I_0(\kappa_{BS})} \frac{1}{2\pi I_0(\kappa_{MS})} \int_{-\pi}^{\pi} \int_{-\pi}^{\pi} \\ &\exp\{-jD_{ss'} \sin(\theta_{i,AoD}^k - \theta_{BS}) \\ &\quad + \kappa_{BS} \cos(\theta_{i,AoD}^k)\} \\ &\exp\{-jD_{uu'} \sin(\theta_{i,AoA} - \theta_{MS}) \\ &\quad + \kappa_{MS} \cos(\theta_{i,AoA} - \bar{\theta}_{AoA})\} \\ &\exp\{\kappa_{BS} \Delta \sin(\theta_{i,AoA}) \sin(\theta_{i,AoD}^k)\} \\ &\exp\{-jD_t \cos(\theta_{i,AoA} - \theta_v)\} d(\theta_{i,AoA}) d(\theta_{i,AoD}^k) \end{aligned} \quad (8)$$

We can often assume that θ_v is an independent variable with uniform distribution over $[0, 2\pi)$. This leads to the well known Bessel function term $J_0(D_t)$ after taking expectation over

θ_v . Therefore the spatial-temporal correlation coefficient after averaging over θ_v is given by

$$\begin{aligned} \rho_{su,s'u'}(\tau) &= \frac{1}{2\pi} \int_{-\pi}^{\pi} \rho_{su,s'u'}(\tau, \theta_v) d\theta_v \\ &\approx J_0(D_t) \frac{1}{2\pi I_0(\kappa_{BS})} \frac{1}{2\pi I_0(\kappa_{MS})} \int_{-\pi}^{\pi} \int_{-\pi}^{\pi} \\ &\exp\{-jD_{ss'} \sin(\theta_{i,AoD}^k - \theta_{BS}) + \kappa_{BS} \cos(\theta_{i,AoD}^k)\} \\ &\exp\{-jD_{uu'} \sin(\theta_{i,AoA} - \theta_{MS}) + \kappa_{MS} \cos(\theta_{i,AoA} - \bar{\theta}_{AoA})\} \\ &\exp\{\kappa_{BS} \Delta \sin(\theta_{i,AoA}) \sin(\theta_{i,AoD}^k)\} d(\theta_{i,AoA}) d(\theta_{i,AoD}^k) \end{aligned} \quad (9)$$

Note that (9) has 4 types of terms. The first term, $J_0(D_t)$, represents average temporal correlation, so that we can isolate the channel temporal behavior from the spatial correlation. The second term is the exponential containing BS parameters which represents spatial correlation at the BS. Similarly, the third term is the the exponential containing MS parameters which represents spatial correlation at the MS. The last term, $\exp\{\kappa_{BS} \Delta \sin(\theta_{i,AoA}) \sin(\theta_{i,AoD}^k)\}$, represents the interaction between AoA and AoD and its effect on the correlation. This is the factor which makes it impossible to separate the spatial correlation into a product of MS and BS terms. Equation (9) gives the full correlation structure for the model.

D. Temporal Correlation Function

Equation (8) shows that for a fixed direction of motion the temporal correlation structure of the channel model is inseparable from the spatial structure and is affected by several parameters. If we look at the temporal correlation at the same antennas ($D_{ss'} = 0$, $D_{uu'} = 0$) and assume Δ is small so that $\kappa_{BS} \Delta \sin(\theta_{i,AoA}) \sin(\theta_{i,AoD}) \approx 0$, then (8) can be approximated as

$$\rho_{su,s'u'}(\tau, \theta_v) \approx \frac{I_0\left(\sqrt{\kappa_{MS}^2 - D_t^2 - 2j\kappa_{MS}D_t \cos(\bar{\theta}_{AoA} - \theta_v)}\right)}{I_0(\kappa_{MS})} \quad (10)$$

Therefore, the temporal correlation given by (10) is related to the AoA distribution and the direction of motion. If the distribution of AoA is isotropic ($\kappa_{MS} = 0$), (10) gives the familiar temporal correlation function $\rho_{su,su}(\tau, \theta_v) = J_0(D_t)$. If the distribution of AoA is nonisotropic ($\kappa_{MS} \neq 0$), the temporal correlation will vary with different directions of motion.

E. Correlation structure based on a series expansion

Computation of (9) requires double numerical integration and for this reason we prefer to investigate approximations based on the series expansion:

$$\begin{aligned} \exp\{\kappa_{BS} \Delta \sin(\theta_{i,AoA}) \sin(\theta_{i,AoD}^k)\} &\approx \\ 1 + \kappa_{BS} \Delta \sin(\theta_{i,AoA}) \sin(\theta_{i,AoD}^k) \end{aligned} \quad (11)$$

We define the zeroth-order and first-order approximations as resulting from taking 1 or 2 terms in the above series

expansion respectively. With these approximations the correlation function in (9) can be simplified considerably using the standard results [3.937, p.488, [16]]

$$\begin{aligned} \int_{-\pi}^{\pi} \exp(p \cos x + q \sin x) dx &= 2\pi I_0(\sqrt{p^2 + q^2}) \\ \int_{-\pi}^{\pi} \exp(p \cos x + q \sin x) \sin x dx &= \\ 2\pi \frac{-q}{\sqrt{p^2 + q^2}} I_1(\sqrt{p^2 + q^2}) \end{aligned} \quad (12)$$

Using (12), the zeroth-order approximation of (9) is

$$\begin{aligned} \rho_{su,s'u'}(\tau) &\approx J_0(D_t) \frac{I_0(\sqrt{p_{BS}^2 + q_{BS}^2})}{I_0(\kappa_{BS})} \frac{I_0(\sqrt{p_{MS}^2 + q_{MS}^2})}{I_0(\kappa_{MS})} \\ &= J_0(D_t) (\mathbf{R}_{BS}^0)_{ss'} (\mathbf{R}_{MS}^0)_{uu'} \end{aligned} \quad (13)$$

and the first-order approximation is

$$\begin{aligned} \rho_{su,s'u'}(\tau) &\approx J_0(D_t) \frac{I_0(\sqrt{p_{BS}^2 + q_{BS}^2})}{I_0(\kappa_{BS})} \frac{I_0(\sqrt{p_{MS}^2 + q_{MS}^2})}{I_0(\kappa_{MS})} \\ &+ J_0(D_t) \left\{ \frac{-\Delta \kappa_{BS} q_{BS}}{\sqrt{p_{BS}^2 + q_{BS}^2}} \frac{I_1(\sqrt{p_{BS}^2 + q_{BS}^2})}{I_0(\kappa_{BS})} \right\} \\ &\times \left\{ \frac{-q_{MS}}{\sqrt{p_{MS}^2 + q_{MS}^2}} \frac{I_1(\sqrt{p_{MS}^2 + q_{MS}^2})}{I_0(\kappa_{MS})} \right\} \\ &= J_0(D_t) [(\mathbf{R}_{BS}^0)_{ss'} (\mathbf{R}_{MS}^0)_{uu'} + (\mathbf{R}_{BS}^1)_{ss'} (\mathbf{R}_{MS}^1)_{uu'}] \end{aligned} \quad (14)$$

where

$$\begin{aligned} p_{BS} &= \kappa_{BS} + j D_{ss'} \sin(\theta_{BS}) \\ q_{BS} &= -j D_{ss'} \cos(\theta_{BS}) \\ p_{MS} &= \kappa_{MS} \cos(\bar{\theta}_{AoA}) + j D_{uu'} \sin(\theta_{MS}) \\ q_{MS} &= \kappa_{MS} \sin(\bar{\theta}_{AoA}) - j D_{uu'} \cos(\theta_{MS}) \end{aligned}$$

and $(\mathbf{R}_{BS}^0)_{ss'}$, $(\mathbf{R}_{BS}^1)_{ss'}$, $(\mathbf{R}_{MS}^0)_{uu'}$, $(\mathbf{R}_{MS}^1)_{uu'}$ are the entries of channel correlation matrix \mathbf{R}_{BS}^0 , \mathbf{R}_{BS}^1 , \mathbf{R}_{MS}^0 , \mathbf{R}_{MS}^1 respectively. I_1 is the first-order modified Bessel function.

F. Channel correlation matrix

For the zeroth order approximation, (13) gives rise to a single-Kronecker result for the channel correlation matrix, $\mathbf{R}_H(\tau) = E(\text{vec}(\mathbf{H}(t)) \text{vec}(\mathbf{H}(t+\tau))^\dagger)$, as below

$$\mathbf{R}_H(\tau) = J_0(D_t) (\mathbf{R}_{BS}^0 \otimes \mathbf{R}_{MS}^0) \quad (15)$$

For the first order approximation a sum-Kronecker form is given:

$$\mathbf{R}_H(\tau) = J_0(D_t) (\mathbf{R}_{BS}^0 \otimes \mathbf{R}_{MS}^0 + \mathbf{R}_{BS}^1 \otimes \mathbf{R}_{MS}^1) \quad (16)$$

In (15) and (16), \otimes is defined as the Kronecker product and the correlation matrices \mathbf{R}_{BS}^0 , \mathbf{R}_{MS}^0 , \mathbf{R}_{BS}^1 , \mathbf{R}_{MS}^1 are Hermitian matrices defined by (13) and (14).

It is interesting that the new model collapses to a single-Kronecker model when the zero order approximation is used and the first order approximation retains the correlation between AoD and AoA via a second Kronecker term. Hence the model encapsulates the AoD-AoA correlation with a logical extension of the single-Kronecker to a sum-Kronecker form and retains a similar concise mathematical structure.

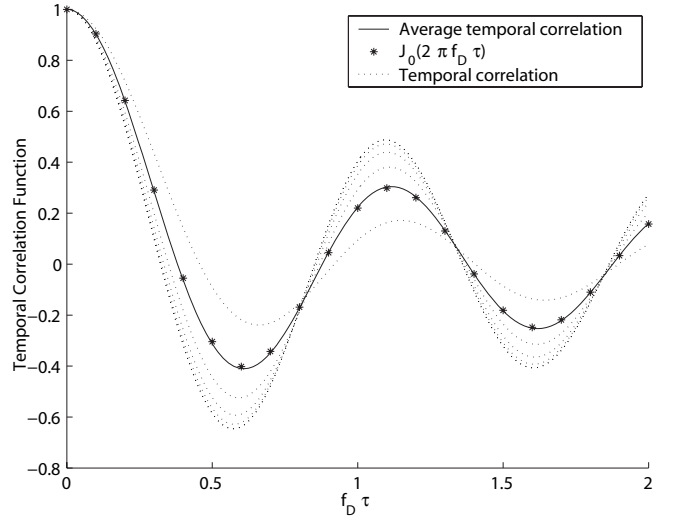


Fig. 2. Temporal correlation function for 5 drops with varied angles of velocity, $D_{ss'} = D_{uu'} = 0$, $\kappa_{MS} = 2$, $\bar{\theta}_{AoA} = 0$.

III. SIMULATION RESULTS

Here we simulate an (n_t, n_r) MIMO system. Unless otherwise stated, we assume that $n_t = n_r = 8$, $\Delta = 2^\circ$, $\bar{\theta}_{AoA} = 0$, $\theta_{BS} = \theta_{MS} = 0$, $d_{ss'} = \lambda$, $d_{uu'} = 0.5\lambda$, $SNR = 20dB$. Two angle spreads are considered at the MS end, $\kappa_{MS} = 0.5$ and $\kappa_{MS} = 3.5$, corresponding to angle spreads of about 88° and 34° which fall in the range of values used in [14]. At the BS end, we use $\kappa_{BS} = 100$ or $\kappa_{BS} = 500$. Simulation of SCM132 [5] for the suburban macro scenario gives a very similar value to $\kappa_{BS} = 100$. These values correspond to an AS of about 6° (for $\kappa_{BS} = 100$) and 3° (for $\kappa_{BS} = 500$). Note that the AS of 6° is at the high end for most practical scenarios. Also, the model loses its physical interpretation for high AS values at the BS, since we assume that $D \gg R$. This corresponds to a small AS and a high value of κ_{BS} . Hence, we restrict ourselves to drawing conclusions in the region $\kappa_{BS} > 100$.

A. Temporal Correlation

Figure 2 shows that when κ_{MS} is non-zero, each different angle of velocity for the MS gives a different temporal correlation function. The five temporal correlation functions shown have velocities with directions randomly selected from a uniform distribution over 360° . When a large number of such uniformly distributed directions is considered, the average temporal correlation function matches the familiar Bessel function as predicted by the theory.

B. Spatial Correlation

Firstly we compare the new sum-Kronecker MIMO model (14) with the one-ring model in [2]. Based on our new model, we have

$$\begin{aligned} \rho_{11,21}(0) &= \frac{I_0(\sqrt{\kappa_{BS}^2 - D_{ss'}^2})}{I_0(\kappa_{BS})} \\ \rho_{11,12}(0) &= \frac{I_0(\sqrt{\kappa_{MS}^2 - D_{uu'}^2})}{I_0(\kappa_{MS})} \end{aligned} \quad (17)$$

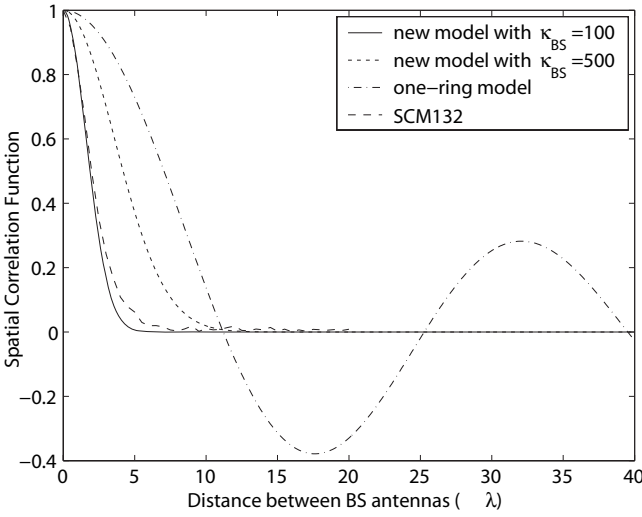


Fig. 3. BS correlation function, $\rho_{11,21}(0)$, for different models vs antenna spacing using default parameters.

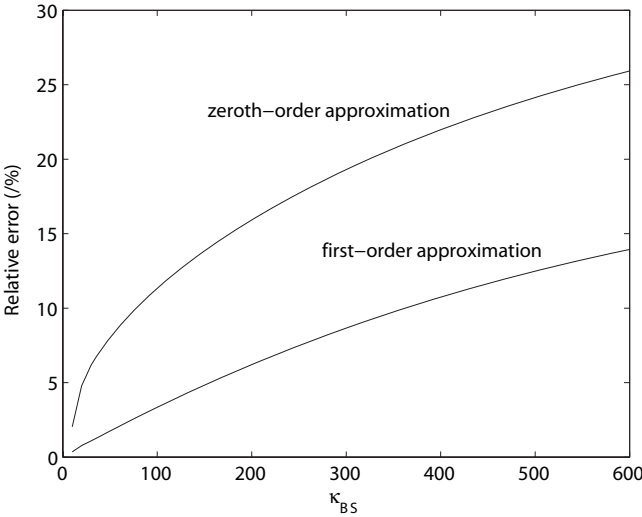


Fig. 4. Relative errors of the zeroth-order and first-order approximation.

whereas the one ring model in [2] gives

$$\begin{aligned}\rho_{11,21}(0) &= \frac{I_0(\sqrt{\kappa_{MS}^2 - D_{ss'}^2 \Delta^2})}{I_0(\kappa_{MS})} \\ \rho_{11,12}(0) &= \frac{I_0(\sqrt{\kappa_{MS}^2 - D_{uu'}^2})}{I_0(\kappa_{MS})}\end{aligned}\quad (18)$$

We can see that the correlation coefficients comparing (17) and (18), $\rho_{11,12}(0)$, are the same at the MS, but $\rho_{11,21}(0)$ is not the same at the BS. Results are shown in Fig. 3 for different BS antenna spacings and κ_{BS} values. The one-ring model shows large oscillating correlations at the BS even for large antenna spacings. The new model suggests that the correlation will decrease roughly exponentially, the speed of decay is related to the value of κ_{BS} and the pronounced oscillations are absent. This type of result agrees with simulations of the SCM132 model [5] and also measured data [17].

C. Approximation Order

In order to show that the zeroth-order and first-order approximations are reasonable, we compare the full correlation (9) (no series expansion) with (13) (the zeroth-order approximation) and (14) (the first-order approximation) in an (8,8) MIMO system. The relative error between an approximated correlation matrix \mathbf{R}_2 and the full correlation matrix \mathbf{R}_1 (without series expansion) is defined as $100 * \|\mathbf{R}_1 - \mathbf{R}_2\| / \|\mathbf{R}_1\|$ where $\|\cdot\|$ is the Frobenius norm. The results are shown in Fig. 4. We can see that the first-order approximation is considerably closer than the zeroth-order approximation and has lower approximation error. It also shows that the larger the value of κ_{BS} , the larger the errors will be. Therefore, a single-Kroneckerstructure is more suited for MIMO systems with small correlation between AoA and AoD and in all cases, a first-order approximation will improve the accuracy of the model. Note that the results in Fig. 4 match typically used values and are physically sensible in the region $\kappa_{BS} > 100$.

D. Ergodic Mutual Information of the MIMO System

If we use a single-Kroneckerstructure (13), the channel matrix is given by

$$\mathbf{H}(t) = (\mathbf{R}_{MS}^0)^{\frac{1}{2}} \mathbf{U}_0(t) (\mathbf{R}_{BS}^0)^{\frac{1}{2}T} \quad (19)$$

where $\mathbf{R}^{\frac{1}{2}}$ is the matrix square root of a Hermitian matrix \mathbf{R} , superscript T denotes transpose and $\mathbf{U}_{(\cdot)}$ is an iid Gaussian channel matrix generated by the Jakes Model with zero mean and unit magnitude variance.

This standard generation method works for the zeroth order approximation as $\mathbf{R}_{(\cdot)}^0$ is Hermitian non-negative definite. For the first order approximation a complication arises since $\mathbf{R}_{(\cdot)}^1$ can have negative eigenvalues. Hence we use an equivalent structure which avoids this problem. Using this approach the channel matrix for the first order approximation is

$$\begin{aligned}\mathbf{H}(t) &= \left(\frac{\mathbf{R}_{MS}^0 - \mathbf{R}_{MS}^1}{\sqrt{2}} \right)^{\frac{1}{2}} \mathbf{U}_0(t) \left(\frac{\mathbf{R}_{BS}^0 - \mathbf{R}_{BS}^1}{\sqrt{2}} \right)^{\frac{1}{2}T} \\ &+ \left(\frac{\mathbf{R}_{MS}^0 + \mathbf{R}_{MS}^1}{\sqrt{2}} \right)^{\frac{1}{2}} \mathbf{U}_1(t) \left(\frac{\mathbf{R}_{BS}^0 + \mathbf{R}_{BS}^1}{\sqrt{2}} \right)^{\frac{1}{2}T}\end{aligned}\quad (20)$$

It can be shown that the matrices of the form $\mathbf{R}_{(\cdot)}^0 \pm \mathbf{R}_{(\cdot)}^1$ may still have negative eigenvalues but they are negligible compared to the other dominant eigenvalues in the Schur decomposition. Hence we can remove them by zeroing these small negative eigenvalues and make the correlation matrices non-negative definite with almost no loss in accuracy.

The EMI of the MIMO system is denoted by \mathcal{I} and is given by

$$\mathcal{I} = E \left\{ \log_2 \left[\det \left(\mathbf{I} + \frac{SNR}{n_t} \mathbf{H} \mathbf{H}^\dagger \right) \right] \right\} \quad (21)$$

where superscript \dagger denotes the transpose conjugate. The EMI difference is defined as the EMI difference between the single-Kronecker and sum-Kroneckerstructures for a MIMO system with specified orientations of the BS and the MS ($\mathcal{I}(\text{single-Kronecker}) - \mathcal{I}(\text{sum-Kronecker})$). When the orientations are uniformly distributed over $[0, 2\pi)$, we can simulate the probability density functions (pdfs) of the EMI difference

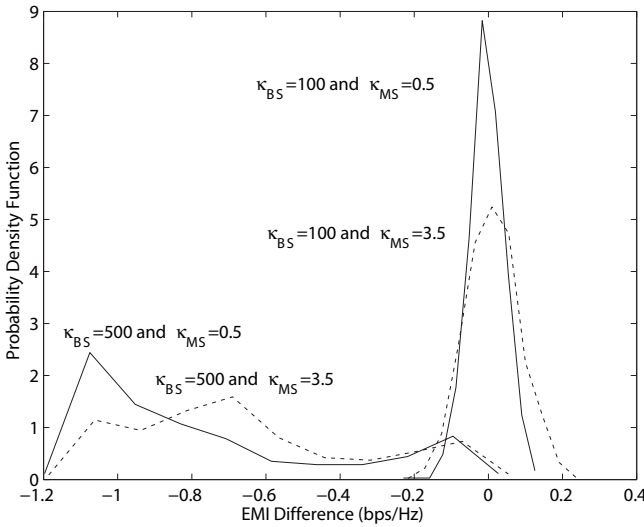


Fig. 5. EMI difference between the single-Kronecker and sum-Kronecker correlation structure.

for different values of κ_{BS} and κ_{MS} as shown in Fig. 5. Each simulated histogram in Fig. 5 is generated from 10,000 channel realizations. The results show that changing κ_{MS} with the same value of κ_{BS} has only a small effect on the location of the EMI difference compared to the BS effects. We also see that the single-Kronecker structure normally underestimates the EMI compared to the sum-Kronecker structure when the correlation of AoA and AoD is large ($\kappa_{BS} = 500$). The higher value of κ_{BS} corresponds to a higher correlation between AoA and AoD. This shows clearly the benefit of the second Kronecker term in the sum-Kronecker correlation structure for the scenarios with correlated AoA and AoD rays. However, when such correlation is small, the sum-Kronecker correlation structure may overestimate or underestimate the EMI with almost equal probability.

The beneficial impact of non-Kronecker channel correlation on MIMO EMI has been reported in [11], [12] but this may be too optimistic. If AoD and AoA are only loosely related, the additional channel correlation may be beneficial or detrimental depending on the orientations of the BS and MS. Hence, in a mobile scenario where no particular orientations are dominant the effect of the non-Kronecker correlation may be negligible. Therefore, the single-Kronecker model tends to systematically underestimate the EMI only when the correlation of AoA and AoD is strong.

IV. CONCLUSION

In this paper we have derived an extension to the popular one-ring model in [1], [2]. The new model allows for varying degrees of correlation between the AoD and AoA of the departing and arriving rays and bridges the gap between Kronecker models and non-Kronecker one-ring models. Approximations to the new model give rise to a zeroth order single-Kronecker approximation and a first order sum-Kronecker approximation. Hence the correlation structure remains mathematically concise for both approximations and

suggests that the sum-Kronecker model may be a sensible general model in non-Kronecker scenarios. Spatial correlations at the BS derived from the new model are substantially different to those in [2] but agree with those in [5]. In particular, the spatial correlation decays smoothly with antenna spacing and is negligible at high spacings. Finally, using the new model we show that non-Kronecker correlation does not necessarily increase the EMI as previously reported. Our results demonstrate that EMI can be increased or decreased depending on the orientation and the correlation between AoA and AoD. Recall, that these conclusions are based on the assumption of a uniformly distributed direction of motion.

REFERENCES

- [1] D. Shiu, G. J. Foschini, M. J. Gans, and J. M. Kahn, "Fading correlation and its effect on the capacity of multi-element antenna systems," *IEEE Trans. Commun.*, vol. 48, no. 3, pp. 502–513, Mar. 2000.
- [2] A. Abdi and M. Kaveh, "A space-time correlation model for multi-element antenna systems in mobile fading channels," *IEEE J. Sel. Areas Commun.*, vol. 20, no. 3, pp. 550–560, Apr. 2002.
- [3] D. Chizhik, J. Ling, P. W. Wolniansky, R. A. Valenzuela, N. Costa, and K. Huber, "Multiple-input-multiple-output measurements and modeling in Manhattan," *IEEE J. Sel. Areas Commun.*, vol. 21, no. 3, pp. 321–331, Apr. 2003.
- [4] K. Yu, M. Bengtsson, B. Ottersten, D. McNamara, P. Karlsson, and M. Beach, "Modeling of wide-band MIMO radio channels based on NLOS indoor measurements," *IEEE Trans. Veh. Tech.*, vol. 53, May 2004.
- [5] 3GPP and 3GPP2, "SCM-132: spatial channel model text description," Apr. 2003.
- [6] P. J. Smith and M. Shafi, "The impact of complexity in MIMO channel models," in *Proc. 2004 IEEE Inter. Conf. on Comm.*, vol. 5, pp. 2924–2928, June 2004.
- [7] T. S. Pollock, "Correlation modelling in MIMO systems: When can we Kronecker?" in *Proc. 5th Australian Comm. Theory Workshop*, pp. 149–153, Feb. 2004.
- [8] H. Özcelik, M. Herdin, W. Weichselberger, J. Wallace, and E. Bonek, "Deficiencies of 'Kronecker' MIMO radio channel model," *Electron. Lett.*, vol. 39, no. 16, pp. 1209–1210, Aug. 2003.
- [9] K. Yu, M. Bengtsson, B. Ottersten, D. McNamara, P. Karlsson, and M. Beach, "Second order statistics of NLOS indoor MIMO channels based on 5.2 GHz measurements," in *Proc. IEEE Global Telecomm. Conf. 2001*, vol. 1, pp. 156–160, Nov. 2001.
- [10] H. Özcelik, M. Herdin, H. Helmut, and E. Bonek, "Capacity of different MIMO systems based on indoor measurements at 5.2 GHz," in *Proc. Personal Mobile Commun. Conf.*, pp. 463–466, 2003.
- [11] C. Oestges and A. J. Paulraj, "Beneficial impact of channel correlations on MIMO capacity," *Electron. Lett.*, vol. 40, no. 10, pp. 606–608, May 2004.
- [12] C. Oestges, B. Clerckx, D. Vanhoenacker-Janvier, and A. J. Paulraj, "Impact of 'diagonal' correlations on MIMO capacity: application to geometrical scattering models," in *Proc. 58th IEEE Vehic. Tech. Conf.*, vol. 1, pp. 394–398, Oct. 2003.
- [13] D. P. McNamara, M. A. Beach, and P. N. Fletcher, "Spatial correlation in indoor MIMO channels," in *Proc. Personal, Indoor and Mobile Radio Commun.*, vol. 1, pp. 290–294, Sept. 2002.
- [14] J. B. A. Abdi and M. Kaveh, "A parametric model for the distribution of the angle of arrival and the associated correlation function and power spectrum at the mobile station," *IEEE Trans. Veh. Technol.*, vol. 51, no. 3, pp. 425–434, May 2002.
- [15] A. Giorgetti, M. Chiani, M. Shafi, and P. J. Smith, "MIMO capacity, level crossing rates and fades: the impact of spatial/temporal channel correlation," *J. Commun. and Networks*, vol. 5, no. 2, pp. 104–115, June 2003.
- [16] I. S. Gradshteyn and I. M. Ryzhik, *Table of Integral, Series, and Products*, corrected and enlarged edition. A. Jeffery Academic Press, 1980.
- [17] W. C. Y. Lee, "Mobile radio signal correlation versus antenna height and spacing," *IEEE Trans. Veh. Technol.*, vol. 25, no. 4, pp. 290–294, Aug. 1977.